http://dx.doi.org/10.5012/bkcs.2013.34.1.95

Temperature-dependent Photoluminescence Study on Aluminum-doped Nanocrystalline ZnO Thin Films by Sol-gel Dip-coating Method

Giwoong Nam,[†] Sang-heon Lee,[‡] Wonshoup So,[‡] Hyunsik Yoon,[†] Hyunggil Park,[†] Young Gue Kim,[†] Soaram Kim,[§] Min Su Kim,[§] Jae Hak Jung,[†,*] Jewon Lee,[†,§] Yangsoo Kim,[†,§] and Jae-Young Leem[†,§,*]

[†]Department of Nano Engineering, Inje University, Gimhae 621-749, Korea. [*]E-mail: jyleem@inje.ac.kr
[‡]School of Chemical Engineering, Yeungnam University, Gyeongsan 712-749, Korea
[§]Department of Nano Systems Engineering, Center for Nano Manufacturing, Inje University, Gimhae 621-749, Korea
[*]E-mail: jhjung@ynu.ac.kr
Received September 10, 2012, Accepted October 8, 2012

The photoluminescence (PT) properties of Al-doped ZnO thin films grown by the sol-gel dip-coating method have been investigated. At 12 K, nine distinct PL peaks were observed at 2.037, 2.592, 2.832, 3.027, 3.177, 3.216, 3.260, 3.303, and 3.354 eV. The deep-level emissions (2.037, 2.592, 2.832, and 3.027 eV) were attributed to native defects. The near-band-edge (NBE) emission peaks at 3.354, 3.303, 3.260, 3.216, and 3.177 eV were attributed to the emission of the neutral-donor-bound excitons (D^0X), two-electron satellite (TES), free-to-neutral-acceptors (e,A^0), donor-acceptor pairs (DAP), and second-order longitudinal optical (2LO) phonon replicas of the TES (TES-2LO), respectively. According to Haynes' empirical rule, we calculated the energy of a free exciton (FX) to be 3.374 eV. The thermal activation energy for D^0X in the nanocrystalline ZnO thin film was found to be ~25 meV, corresponding to the thermal dissociation energy required for D^0X transitions.

Key Words : II-VI, Luminescence

Introduction

In recent decades, investigations for blue and UV photonics have become the focus of interest. The preparation of the first GaN-based light-emitting diode with emission was achieved in 1993. ZnO is a potential competitor of GaN for blue and UV light-emitter and detector application, and also high-power, high-frequency electronic devices.[1] ZnO with a band gap of 3.4 eV has become a natural choice considering its low toxicity and abundance in the earth. ZnO is characterized by a large exciton binding energy (~60 meV), as compared to the 26 meV exciton binding energy in GaN, which allows the stable existence of excitons and deficient excitonic lasing operation at room temperature or even higher. Moreover, ZnO is a multifunctional semiconductor material that has been exploited for short-wavelength optoelectronic applications such as light-emitting diodes, laser diodes, photodetectors, *etc.*.[25] To enhance its optical properties, ZnO is commonly doped with Group III elements (B, In, Al, or Ga). ZnO thin films have been prepared by a variety of thin-film deposition techniques, such as pulsed-laser deposition,[6] RF magnetron sputtering,[7] chemical vapor deposition,[8] spray pyrolysis,[9] chemical bath deposition,[10] and the sol-gel process.[11-13] Among the preparation techniques of ZnO thin films, the sol-gel process in combination with the dip-coating process offers the greatest possibility for low-cost small and large-area coating of ZnO thin films for technological applications. Despite extensive research over the past several years, some fundamental properties of the low-temperature photoluminescence (PL) in ZnO by sol-gel dip-coating are still not fully understood.

We carried out a detailed study on the PL emanating from Al-doped nanocrystalline ZnO thin film grown on a quartz substrate in the temperature range of 12-180 K. Spectra pertaining to free excitons (FX), neutral-donor-bound excitons (D^0X), donor-acceptor pairs (DAP) transitions, free-to-neutral-acceptors (e,A^0), two-electron satellites (TES) and their longitudinal optical (LO) phonon replicas were identified and analyzed.

Experimental Details

An Al-doped crystalline ZnO thin film was deposited on the quartz substrate using a sol-gel dip-coating process. The sol was prepared using zinc acetate dehydrate ($Zn(CH_3COO)_2 \cdot 2H_2O$), aluminum nitrate nonahydrate ($Al(NO_3)_3 \cdot 9H_2O$), 2-methoxyethanol ($C_3H_8O_2$), and monoethanolamine (C_2H_7NO, MEA). The zinc acetate dehydrate and aluminum nitrate nonahydrate were dissolved in 2-methoxyethanol, and then MEA was added to the solution as a stabilizer. The concentration of metal ions in the solution was 0.3 mol/L (Al/Zn = 3 at.%). The molar ratio of MEA to metal salts was 1.0, and the ratio of Al to Zn was fixed at 3 at.%. The mixed solution was stirred at 60 °C for 2 h until it became clear and homogeneous. It was cooled to room temperature and aged for 24 h before using it as the coating solution for deposition.

The quartz substrate was ultrasonically cleaned in acetone and ethanol for 10 min and then rinsed with de-ionized water and dried by blowing nitrogen. The Al-doped nanocrystalline ZnO thin film was dip-coated onto the quartz substrate at a

lifting speed of 8 cm/min under computer-controlled dipping parameters. After deposition by dip-coating, the films were dried in an oven at 150 ºC for 10 min to evaporate the solvent and remove organic residuals. The dip-coating and pre-heating procedures were carried out five times. The films were then post-heated in the furnace at 500 ºC for 1 h.

The luminescent properties of the Al-doped nanocrystalline ZnO thin film were investigated through PL measurements using a He-Cd laser (325 nm) with an excitation power of 20 mW and a 0.75-m single-grating monochromator with a photomultiplier tube over a wide temperature range of 12-180 K.

Results and Discussion

Figure 1 shows the PL spectrum of the nanocrystalline ZnO thin film at low temperature (12 K) and the draft of the anticipated level of defect in the nanocrystalline ZnO thin film. At 12 K, nine distinct PL peaks were observed at 2.037, 2.592, 2.832, 3.027, 3.177, 3.216, 3.260, 3.303, and 3.354 eV. The deep-level (DL) emissions (2.037, 2.592, 2.832, and 3.027 eV) were attributed to native defects. The peaks at 2.037 and 3.027 eV were attributed to interstitial oxygen (O_i)[14,15] and a zinc vacancy (V_{Zn}),[16] respectively. We supposed that the peak at 2.832 eV was probably due to a high exciton binding energy of 60 meV or interstitial aluminum (Al_i). In Figure 1(b), the peak at 2.592 eV was generated by V_{Zn} and above proposal. The near-band-edge (NBE) emission peaks at 3.354, 3.303, 3.260, and 3.216 eV were attributed to the emission of D^0X,[17] TES,[18] (e,A^0),[19] and DAP,[20] respectively. The other peak at 3.177 eV, which correspond to the TES-2LO are obtained from the fittings. Highly polar semiconductors such as ZnO are known for their significant exciton-phonon coupling. It is a well-known fact that the LO phonon replicas of TES in ZnO have been generally identified through the energy interval between a TES peak and the LO phonon energy ($\hbar\omega = 70$ meV). In the LO phonon replicas of TES, the TES-1LO was not found, because the intensity of this peak was weak or this energy was freed by the DAP. The energy interval between the TES and TES-2LO was 126 meV, which was less low 144 meV, as shown in Figure 1(a). The peak at 3.303 eV can be resolved into TES,[18] DAP,[21] exciton-exciton scattering,[22] and first-order longitudinal optical (1LO) phonon replicas of the FX and D^0X. The peak at 3.303 eV could be attributed to TES. Bound excitons are extrinsic transitions and are related to dopants or defects, which usually create discrete electronic states in the band gap. In theory, excitons could be bound to neutral or charged donors and acceptors. The neutral shallow donor-bound exciton often dominates because of the presence of donors from unintentional impurities and/or shallow donor-like defects. Another characteristic of the D^0X transition is a TES transition. During the recombination of D^0X, the final state of the donor can be a 1s (normal D^0_iX line) or 2s/2p state (TES_i line). The energy between the D^0_iX and its TES_i is the difference between the donor energies in the 1s and 2s/2p states. The donor excitation energy from the ground state to the first excited state is equal to 3/4 of the donor binding energy (E_D). According to the peak positions of the TES and D^0X, we calculated E_D as 68 meV. According to Haynes' empirical rule,[23] E_D can be expressed as

$$E_D = (E_{FX} - E_{D^oX})/\alpha, \quad (1)$$

where E_{FX} is the FE transition energy, E_D0_X is the energy of D^0X, and α is the Haynes' factor (0.3). This implies that the exciton-donor binding energy is proportional to E_D. According to Haynes' empirical rule, we calculated the energy of FX as 3.374 eV. The acceptor binding energy E_A is given by

$$E_{(e,A^0)} = E_g - E_A + k_B T/2, \quad (2)$$

where E_g is the band gap and k_B is Boltzmann's constant. If we use the value of $E_g = 3.437$ eV at 12 K,[24] we can obtain an E_A value of ~178 meV.

Figure 2 shows the temperature dependence of the PL

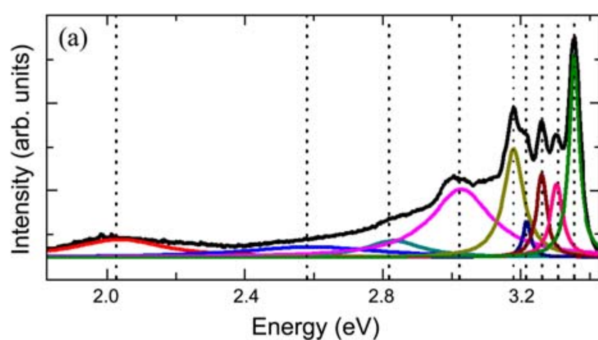

Figure 1. (a) PL spectrum of the nanocrystalline ZnO thin film at 12 K and (b) the draft of the anticipated level of defect in nanocrystalline ZnO thin film.

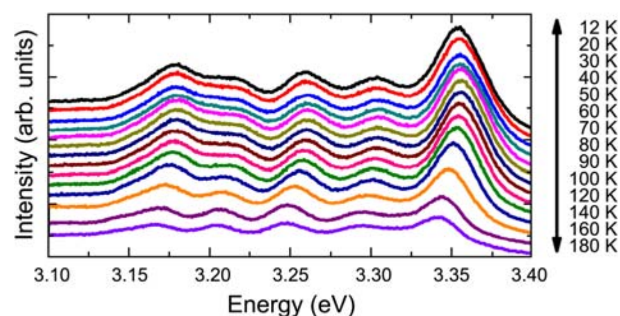

Figure 2. Temperature-dependent PL spectra of NBE emissions of nanocrystalline ZnO thin film grown on quartz substrate.

spectra for nanocrystalline ZnO thin film between 3.10-3.40 eV within a temperature range of 12-180 K. In general, the D^0X emission is dominant at low temperatures. In particular, because of the abundance of D^0X in ZnO, the photon emissions FX and D^0X are usually mixed. As the temperature increases, the emission of FX becomes dominant, and localized carriers are thermalized to occupy higher energy states, which leads to a blueshift in D^0X, TES, (e,A^0), and DAP. This blueshift behavior is observed in the temperature range 12 K < T < 50 K. With increasing temperature, the DAP emission energy was redshifted in the temperature range 50 K < T < 180 K. For a DAP transition, the energy of the photon resulting from radiative recombination is given by

$$h\nu = E_g - E_A - E_D + \frac{q^2}{\varepsilon r}, \quad (3)$$

where E_g is the band gap, E_A and E_D are the acceptor and donor binding energies, respectively, ε is the dielectric constant, and r is the donor-acceptor distance. With increasing temperature, carriers on DAP with small distance r are released into the band, and the line is shifted to the low-energy side. The peak at 3.354 eV is redshifted with increasing temperature. With an increase in temperature, the thermal energy (kT) protects the exciton localization energy, and the lineshape of the emission peak becomes the characteristic line shape of FX recombination, producing the redshift characteristic of temperature dependence of the band-gap energy of semiconductor materials. The FX is generally too weak to be easily identified because of the localization of excitons by impurities, particularly by donors or acceptors.[25]

The temperature-dependent D^0X transition energy can be fitted by Cody's equation:

$$E_g(T) = E_g(0) - k/[\exp(\theta/T) - 1] \quad (4)$$

where E_g is the band gap energy and k is a constant. The parameter θ is related to the average phonon frequency, and it can be represented by the Einstein temperature θ_E. The experimental data were also fitted with $E_g(0) = 3.354$ eV, $k = 0.18$ eV, and θ = 500 K as shown in Figure 3. The experimental curve does not agree in the temperature range 12 K < T < 80 K, because the localized carriers occupy higher energy states. However, at temperature above 80 K the

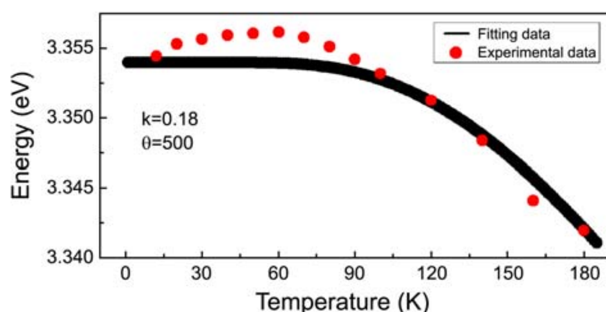

Figure 3. Peak energy for D^0X as a function of temperature. Solid lines indicate fitting of experimental data using Eq. (4).

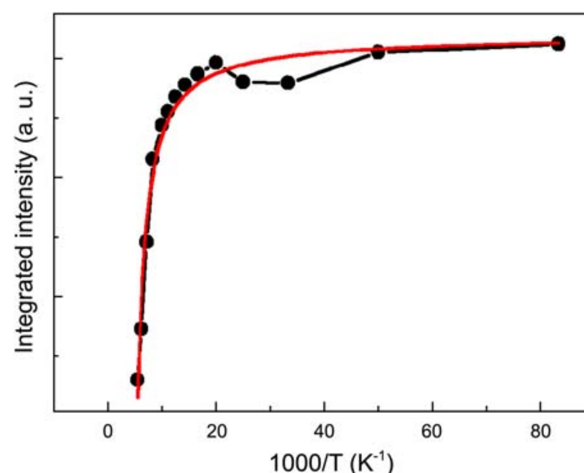

Figure 4. Integrated PL intensity dependence on temperature. Solid line is fit to experimental data using Eq. (5).

temperature dependence of the PL peak position agrees well with Cody's equation.

Moreover, the integrated PL intensity of the D^0X peak was expressed as a function of the inverse temperature, as shown in Figure 4. It was observed that the intensities decayed with temperature increase in agreement with the following expression:

$$I = \frac{I_0}{[1 + C\exp(-\Delta E_A/k_B T)]}, \quad (5)$$

where I_0 is the intensity at $T = 0$ K, C is the ratio of non-radiative transition probability, k_B is Boltzmann's constant, and ΔE_A is the thermal activation energy for thermal quenching. The thermal activation energy for a bound exciton is directly linked to E_{loc}, the energy required to remove an exciton from the defects.[26] Eq. (5) assumes that the dominant mechanism for the PL intensity change with increasing temperature is the thermal activation of carriers. The thermal activation energy for the D^0X with increasing temperature in the nanocrystalline ZnO thin film was found to be ~25 meV, corresponding to the thermal dissociation energy required for the D^0X transitions. The PL intensity is normally observed to decrease monotonically with increasing temperature, which is called the "thermal quenching" phenomenon. However, as seen in Figure 4, the PL shows increasing intensity with rising temperature in the range 30 K < T < 50 K. This temperature dependence is unusual and called the "negative thermal quenching" phenomenon, which is a characteristic sign of the contribution of intermediate states to the recombination process.[27]

Conclusion

We report temperature-dependent PL studies on Al-doped ZnO thin films grown by the sol-gel dip-coating method. At 12 K, nine distinct PL peaks were observed at 2.037, 2.592, 2.832, 3.027, 3.177, 3.216, 3.260, 3.303, and 3.354 eV. The DL emissions (2.037, 2.592, 2.832, and 3.027 eV) were

attributed to native defects. The near-band-edge (NBE) emission peaks at 3.354, 3.303, 3.260, 3.216, and 3.177 eV were attributed to the emission of D^0X, TES, (e,A^0), DAP, and the TES-2LO, respectively. According to the peak positions of the TES and D^0X, we calculated E_D as 68 meV. According to Haynes' empirical rule, we calculated the energy of FX as 3.374 eV. The temperature-dependent D^0X transition energy was fitted by Cody's equation. The experimental data were also fitted with $E_g(0) = 3.354$ eV, $k = 0.18$ eV, and $\theta = 500$ K. The thermal activation energy for the D^0X in the nanocrystalline ZnO thin film was found to be ~25 meV, corresponding to the thermal dissociation energy required for the D^0X transitions.

Acknowledgments. This research was supported by Basic Science Research Program Through the National Research Foundation of Korea (NRF) funded by the Ministry of Education, Science and Technology (No. 2012R1A1B3001837). This research was supported by Basic Science Research Program through the National Research Foundation of Korea (NRF) funded by the Ministry of Education, Science and Technology (Grant Number 2012-0008002). This study was supported by the Human Resources Development Program of Korea Institute of Energy Technology Evaluation and Planning (KETEP) grant (No 20104010100580) funded by the Korean Ministry of Knowledge Economy.

References

1. Look, D. C. *Mater. Sci. Eng. B* **2001**, *80*, 383.
2. Huang, M. H.; Mao, S.; Feick, H.; Yan, H. Q.; Wu, Y. Y.; Kind, H.; Weber, E.; Russo, R.; Yang, P. D. *Science* **2001**, *292*, 1897.
3. Hoffman, R. L.; Norris, B. J.; Wager, J. F. *Appl. Phys. Lett.* **2003**, *82*, 733.
4. Liu, K. W.; Ma, J. G..; Zhang, J. Y.; Lu, Y. M.; Jiang, D. Y.; Li, B. H.; Zhao, D. X.; Zhang, Z. Z.; Yao, B.; Shen, D. Z. *Solid-State Electron.* **2007**, *51*, 757.
5. Liu, K. W.; Shen, D. Z.; Shan, C. X.; Zhang, J. Y.; Yao, B.; Zhao, D. X.; Lu, Y. M.; Fan, X. W. *Appl. Phys. Lett.* **2007**, *91*, 201106.
6. Hayamizu, S.; Tabata, H.; Tanaka, H.; Kawai, T. *J. Appl. Phys.* **1996**, *80*, 787.
7. Anna Selvan, J. A.; Keppner, H.; Shah, A. *Mater. Res. Soc. Symp. Proc.* **1996**, *426*, 497.
8. Deschanvres, J. L.; Bochu, B.; Joubert, J. C. *J. Phys.* **1993**, *4*, 485.
9. Messaoudi, C.; Sayah, D.; Abd-Lefdil, M. *Phys. Status Solidi* **1995**, *151*, 93.
10. O'Brien, P.; Saeed, T.; Knowles, J. *J. Mater. Chem.* **1996**, *6*, 1135.
11. Schuler, T.; Aegerter, M. A. *Thin Solid Films* **1999**, *351*, 125.
12. Kamalasanan, M. N.; Chandra, S. *Thin Solid Films* **1996**, *288*, 112.
13. Jiménez González, A. E.; Soto Urueta, J. A. *Sol. Energy Mater. Sol. Cells* **1998**, *52*, 345.
14. Srikant, V.; Clarke, D. R. *J. Appl. Phys.* **1998**, *83*, 5447.
15. Goldsmith, S. *Surf. Coat. Technol.* **2006**, *201*, 3993.
16. Fan, X. M.; Lian, J. S.; Zhao, L.; Liu, Y. H. *Appl. Surf. Sci.* **2005**, *252*, 420.
17. Jie, J.; Wang, G.; Han, X.; Fang, J.; Xu, B.; Yu, Q.; Liao, Y.; Li, F.; Hou, J. G. *J. Crystal Growth* **2004**, *267*, 223.
18. Petersen, J.; Brimont, C.; Gallart, M.; Cregut, O.; Schmerber, G.; Gilliot, P.; Honerlage, B.; Ulhaq-Bouillet, C.; Rehspringer, J. L.; Leuvrey, C.; Colis, S.; Slaoui, A.; Dinia, A. *Microelectr. J.* **2009**, *40*, 239.
19. Pan, X. H.; Jiang, J.; Zeng, Y. J.; He, H. P.; Zhu, L. P.; Ye, Z. Z.; Zhao, B. H.; Pan, X. Q. *J. Appl. Phys.* **2008**, *103*, 023708.
20. Pfisterer, D.; Sann, J.; Hofmann, D. M.; Plana, M.; Neumann, A.; Lerch, M.; Meyer, B. K. *Phys. Stat. Sol. (b)* **2006**, *243*, R1.
21. Qiu, J.; Li, X.; He, W.; Park, S.-J.; Kim, H.-K.; Hwang, Y.-H.; Lee, J.-H.; Kim, Y.-D. *Nanotechnology* **2009**, *20*, 155603.
22. Su, S. C.; Lu, Y. M.; Xing, G. Z.; Wu, T. *Superlattice Microst.* **2010**, *48*, 485.
23. Ozgur, U.; Alivov, Ya. I.; Liu, C.; Teke, A.; Reshchikov, M. A.; Dogan, S.; Avrutin, B.; Cho, S.-J.; Morkoc, H. *J. Appl. Phys.* **2005**, *98*, 041301.
24. Look, D. C. *Mater. Sci. Eng. B* **2001**, *80*, 383.
25. Yang, X. D.; Xu, Z. Y.; Sun, Z.; Sun, B. Q.; Ding, L.; Wang, F. Z.; Ye, Z. Z. *J. Appl. Phys.* **2006**, *99*, 046101.
26. Dietrich, C. P.; Brandt, M.; Lange, M.; Kupper, J.; Bontgen, T.; von Wenckstern, H.; Grundmann, M. *J. Appl. Phys.* **2011**, *109*, 013712.
27. Shibata, H. *Jpn. J. Appl. Phys.* **1998**, *37*, 550.